JOURNAL OF PLASTIC SURGERY AND HAND SURGERY
2024, VOL. 59, 162–170
https://doi.org/10.2340/jphs.v59.42322

ORIGINAL RESEARCH ARTICLE

Variations in orbital morphology, globe:orbit volume relation, and ophthalmological outcome in unicoronal synostosis

Hanna M. Lif, MD[a]*, Evangelia Ntoula, MD[b]*, Eva Larsson, MD PhD[b]** and Daniel J. Nowinski, MD, PhD[a]**

[a]Department of Surgical Sciences, Plastic Surgery, Uppsala University, Uppsala, Sweden; [b]Department of Surgical Sciences, Ophthalmology, Uppsala University, Uppsala, Sweden

ABSTRACT

Nonsyndromic unicoronal synostosis is associated with variability of severity in orbital morphology and ophthalmological manifestations. The relation between the two is not fully understood, nor how surgical treatment with fronto-orbital advancement and remodelling (FOAR) changes the relation. The aim of this study was to elucidate associations between ophthalmological manifestations and variations in orbital morphology and globe:orbit volume ratios preoperatively and at long-term follow-up after surgery. Twelve children referred to Uppsala Craniofacial Center who underwent computed tomography and standardized ophthalmological examinations regarding strabismus, spherical equivalent, astigmatism, anisometropia, and subnormal vision preoperatively and at 3 years of age were included. Orbits and globes were segmented. Principal component analysis elucidated morphological variation, and symmetry between orbital pairs was measured as the Dice similarity coefficient and globe:orbit volume ratios were calculated. The defined orbital shape variations were correlated with strabismus, refractive error, and subnormal vision. Different shape variations were associated with strabismus pre- and postoperatively and ipsi- and contralateral astigmatism. Greater improvement in orbital symmetry after surgery was associated with improvement in astigmatic anisometropia and new onset strabismus at follow-up. A small globe:orbit volume ratio was associated with preoperative strabismus, while the opposite was seen at follow-up. Different mechanisms seem to cause strabismus pre- and postoperatively, and FOAR might not sufficiently correct orbital morphology.

ARTICLE HISTORY
Received 3 June 2024
Accepted 21 October 2024
Published 12 December 2024

KEYWORDS
Nonsyndromic unicoronal synostosis; surgical outcome; ophthalmological outcome; orbital symmetry; globe volume; imaging

Introduction

Nonsyndromic unicoronal synostosis (UCS) is the third most common single-suture craniosynostosis and is associated with variable morphological and functional outcomes. Ophthalmological disorders such as astigmatism, anisometropia, and strabismus are well described in the literature [1–8]. Previous studies have suggested associations between orbital morphology and ophthalmological disorders [1, 5, 9]. However, the causes of ophthalmological disorders in UCS as well as the relation between morphology and functional outcome are yet to be fully understood.

There are several surgical treatment approaches in UCS. The choice of surgical treatment is traditionally not individualized based on patient-specific factors but rather dictated by surgical protocols where each center usually offers one treatment approach. Fronto-orbital advancement and remodelling (FOAR) is the most common surgical treatment for UCS [7, 9–11]. In principle, the forehead and supraorbital rim are corrected bilaterally. Advancement of the ipsilateral supraorbital frame and forehead is a fundamental aspect of FOAR. Overcorrection serves to prohibit relapse of the deformity with skull growth. It appears that FOAR may induce strabismus in a fraction of patients [7, 8, 12], but the mechanisms behind why it affects some patients and not others are unknown. Therefore, there is a need to investigate relations between pre- and postoperative orbital morphology and ophthalmological outcomes in order to enhance the knowledge on how to prevent functional dysfunctions in UCS and optimize surgical treatment. The impact of change in orbital morphology after FOAR on subsequent ophthalmological dysfunctions is largely unknown [9].

Previous studies on craniosynostosis have used statistical shape modeling including the Dice similarity coefficient (Dice) to determine the severity of orbital asymmetry based on computed tomography (CT) images [13–15]. Principal component analysis (PCA) has been used to quantify variation in morphology in craniosynostosis patients [13, 16–20], enabling analyses of correlation between morphological variation and outcome. The globe and its relation to the orbit have previously been investigated in craniosynostosis syndromes [21], but to our knowledge not in UCS. Overall, there is a lack of studies objectively investigating the relation between morphology and function in UCS [11]. The aim of this study was to elucidate associations between ophthalmological manifestations and variation in orbital morphology, globe:orbit volume, and improvement in orbital symmetry, preoperatively, and at long-term follow-up after surgical intervention.

Material and methods

Patients referred to Uppsala Craniofacial Center, Uppsala University Hospital, Sweden for nonsyndromic UCS were included. All patients underwent surgical treatment with FOAR, preferably scheduled at 10 months of age. A previous study has described the procedure [13].

CONTACT Evangelia Ntoula evangelia.ntoula@uu.se Department of Surgical Sciences/Ophthalmology, Uppsala University, S-751 85 Uppsala, Sweden
* Shared first authorship; ** Shared last authorship.

© 2024 The Author(s). Published by MJS Publishing on behalf of Acta Chirurgica Scandinavica. This is an Open Access article distributed under the terms of the Creative Commons Attribution 4.0 International License (http://creativecommons.org/licenses/by/4.0/), allowing third parties to copy and redistribute the material in any medium or format and to remix, transform, and build upon the material, with the condition of proper attribution to the original work.

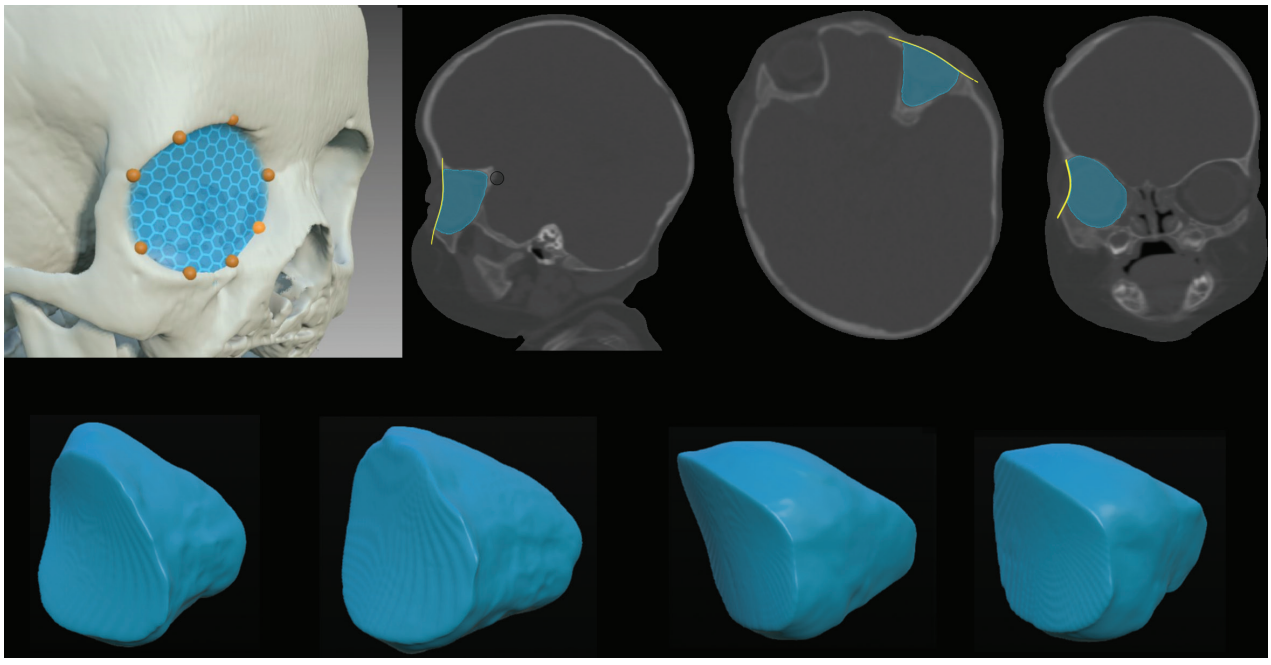

Figure 1. Segmentation of orbits. Eight landmarks were placed on the anterior rim of the orbit to calculate a mesh defining the anterior border of the orbit. Then, voxels of the orbit were semi-automatically segmented resulting in a 3D representation of orbital shape on which further image analyses were based.

Genetic panels were performed on all patients and identified mutations led to exclusion. Information about craniosynostosis, results from genetic panels, ophthalmological examinations, age at surgery, and examinations were collected from medical records. CT and ophthalmological examinations were performed as part of our center's protocolized multidisciplinary assessment for craniosynostosis patients. Preoperatively, CT and examination by an experienced pediatric ophthalmologist and orthoptist were performed. Follow-up CT was conducted at 3 years of age. Standardized ophthalmological follow-up was scheduled at age 3 and 5 by a pediatric ophthalmologist and orthoptist. If complete ophthalmological examinations were performed at both ages, the latest was included in the study. Only patients with complete data and adequate CT quality both preoperatively and at follow-up were included. The main reason for exclusion was lack of standardization of CT examinations performed at referring hospitals. Therefore, 11 patients operated with FOAR were excluded from the study, 9 due to inadequate imaging of both orbits pre- or postoperatively, 1 due to an identified mutation, and 1 had not yet reached 3 years by the time of the study. Collected data were divided into four groups: preoperative ipsilateral, preoperative contralateral, follow-up ipsilateral, and follow-up contralateral.

Ophthalmological outcome

Included outcomes in the study were strabismus, spherical equivalent (SE), astigmatism, anisometropia, and subnormal vision. The visual and refractive outcome and orthoptic measurements preoperatively and at age 3 or 5 were assessed. Preoperatively, visual acuity was measured with the Preferential Looking test (Teller Acuity Cards or Cardiff Cards) monocularly and binocularly, or in children too young to cooperate, with observation of fixation and following. Subnormal vision was considered the inability to fix and follow a 5 cm target at a distance of 30 cm or considered subnormal according to the manuals of Preferential Looking tests. At follow-up examinations at 3 and 5 years, LogMar optotypes (Lea or HVOT) were used. Vision was considered subnormal when >0.3 and >0.1 LogMar, respectively (<0.5 and <0.8 Snellen decimal acuity).

The refraction was measured in cycloplegia after the instillation of eye drops including cyclopentolate 0.5% and phenylephrine 0.5% in children under 1 year of age and drops including cyclopentolate 1.5% and phenylephrine 0.85% in older children. The cylindrical value and axis of astigmatism were noted. SE was considered the merging of the spherical and cylindrical refractive error and calculated by adding the sphere power with half of the cylinder power. Hypermetropia was defined as SE ≥2.0 diopter (D). Astigmatism was recorded as a negative cylinder, and astigmatism axis was divided as with the rule (0°–15° or 165°–180°), against the rule (75°–105°), or oblique (16°–74° or 106°–164°). Astigmatism was considered significant if ≥1.0 D. Astigmatic anisometropia and anisometropia of SE were defined as the difference of values between the two eyes and were considered significant if ≥1.0 D in both cases. Manifest or intermittent strabismus, type, and side of deviation as well as eye motility were noted.

Morphology and volume

The Picture Archiving Communication System Vue Motion (Carestream) was used to collect CT dicom data. Orbital voxels were semi-automatically segmented in the software OrbSeg 0.9.3 as previously described [13, 22] (Figure 1). In summary, voxels of the orbital volume were semi-automatically segmented using a 3D brush that paints in multiple layers simultaneously without including other structures as it interprets the limitation of the orbital wall based on Hounsfield units and respects the anterior border as it is defined by a mesh created from eight landmarks defining the anterior border of the orbit before segmentation. Ipsilateral orbits were then mirrored and aligned to enable comparison between orbital pairs (Figure 2), as described by a flowchart in a previous study [13]. In short, after centroid matching, iterative closest point registration and Generalized Procrustes Analysis were conducted to ensure sufficient alignment. Morphological analyses were performed using the programming language Python and consisted of two primary analyses on segmented

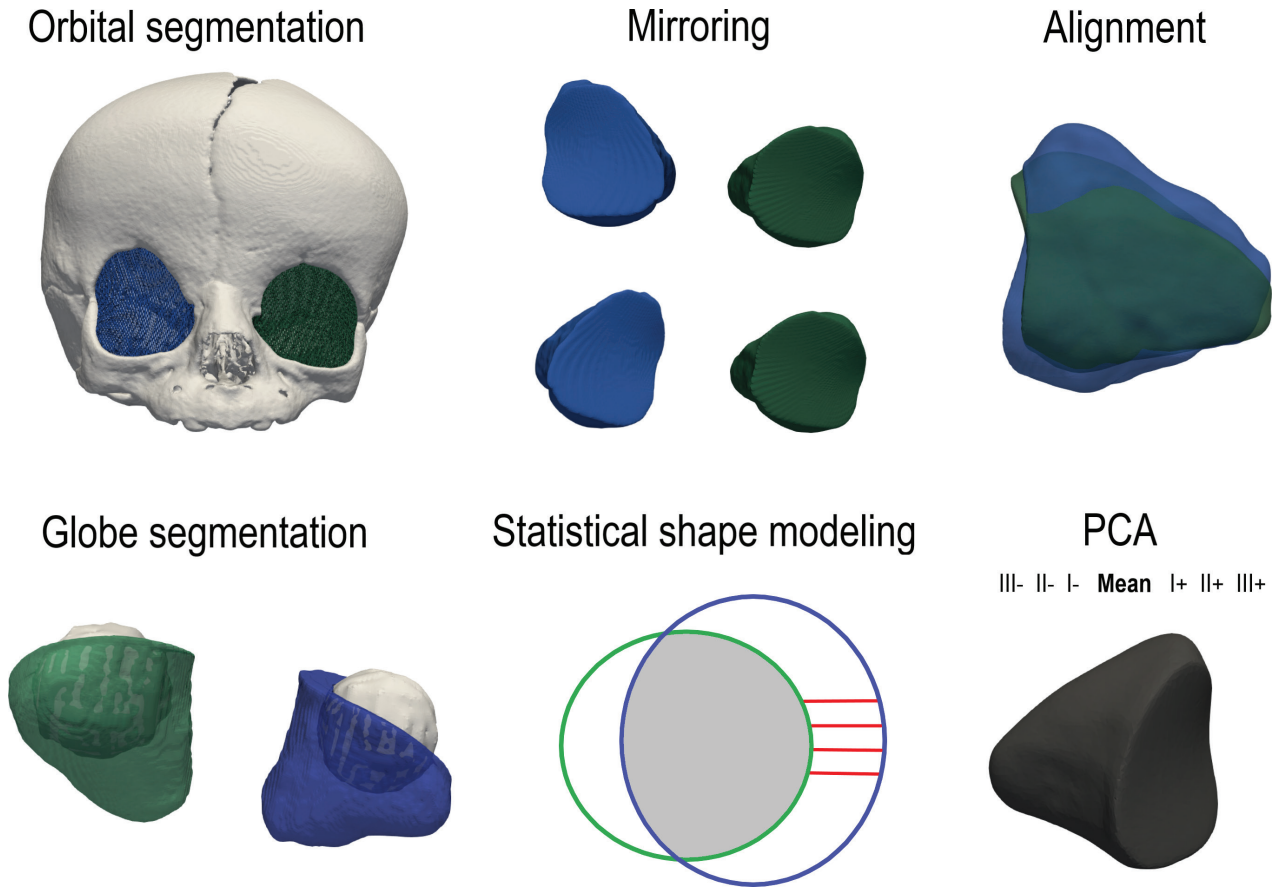

Figure 2. Workflow of image analysis. Segmentation of the ipsi- (blue) and contralateral (green) orbits, followed by mirroring and alignment. Separate segmentation of the globe. Statistical shape modeling by symmetry calculated as the Dice illustrated by the gray area between two aligned shapes (blue and green), and measurements to create signed distance maps illustrated by red lines measured between vertices of the aligned shapes. The principle of principal component analysis is illustrated with the different included modes and visualized mean model of one group. Dice: Dice similarity coefficient; PCA: principal component analysis; I+: positive first principal mode; I-: negative first principal mode; II+: positive second principal mode; II-: negative second principal mode; III+: positive third principal mode; III-: negative third principal mode.

orbits: calculation of orbital symmetry as Dice and PCA (Figure 2), which have been described in detail in a previous study [13]. To segment the globe, segmented orbits were visualized in ITK-SNAP (Insight Segmentation and Registration Toolkit SNAP) [23], and an additional label was used for separate segmentation of the globe on CT slices using a 3D isotropic brush in axial, coronal, and sagittal views (Figure 2). Volumes of the globe and of the orbit without the globe were calculated in ITK-SNAP. The globe:orbit volume ratio was calculated as the ratio between the globe and the total volume (globe+orbit). To quantify symmetry, Dice was calculated for each orbital pair, resulting in a value between 0 and 100% where 100% equals perfect symmetry. Improvement in symmetry was determined as the difference in Dice between the preoperative and follow-up CT.

Coloured distance maps for individual patients were based on minimal and maximal Hausdorff distances between vertices (Figure 2), which were calculated in MeshLab 2022.02 (ISTI – CNR research center). Hausdorff distances describe difference between surfaces, as opposed to Dice that calculates differences between voxels. These visualized morphological differences between ipsi- and contralateral sides preoperatively and at follow-up by illustrating the ipsilateral morphology and adding how the contralateral morphology differed from it.

Regarding variability in morphology, PCA was performed on each of the four groups and enabled statistically summarizing large data for visualization and interpretation. Since UCS is a highly variable condition, a very large number of principal components would be required to explain all of the variance. Inclusion of all principal components would make it impossible to interpret the results and connect them to functional data in a meaningful way. Therefore, only shapes explaining most of the variation were considered and analyzed: the first (PC1), second (PC2), and third (PC3) principal components. Each principal component represented a morphological spectrum between negative and positive aspects, resulting in six different illustrations of shapes for each group: PC1-, PC1+, PC2-, PC2+, PC3-, and PC3+. Although present, aspects of size from the PCA were not taken into consideration, only morphology. To interpret which morphological variation each orbit was mostly associated with, the first, second, and third principal component coefficients were calculated using the following equation:

$$orbit \approx orbit_{mean} + PC_1 shape\ mode_1 + PC_2 shape\ mode_2 + PC_3\ shape\ mode_3 = orbit_{mean} + b_1\sqrt{\lambda_1 e_1} + b_2\sqrt{\lambda_2 e_2} + b_3\sqrt{\lambda_3 e_3}$$

Morphology, volume, and ophthalmological outcome

The difference in Dice preoperatively and at age 3 was related to differences in anisometropia and strabismus preoperatively and at age 3 or 5. For each of the four groups, the relation between PC1, PC2, PC3 preoperatively and at age 3, respectively, and strabismus, astigmatism, SE, and subnormal vision preoperatively and at age 3 and 5 was investigated.

Table 1. Ages, ophthalmological status, symmetry, and globe:orbit volume ratio preoperatively and at follow-up.

Variables	Preoperative	Follow-up
Mean age at ophthalmological examination	10 ± SD 3 (range 3–26) months	4.2 ± SD 1 (range 3.1–5.4) years
Mean age at CT	10 ± SD 5 (range 4–22) months	3.1 ± SD 0.3 (range 2.7–3.7) years
Strabismus	Ipsilateral: 0/12	Ipsilateral: 4/12 Vertical: 4
	Contralateral: 3/12 Vertical: 1 Exotropia: 2 Esotropia: 1	Contralateral: 6/12 Vertical: 1 Exotropia: 4 Esotropia: 2
SE ≥ 2D	Ipsilateral: 8/12	Ipsilateral: 6/12
	Contralateral: 8/12	Contralateral: 5/12
Astigmatism ≥ 1D	Ipsilateral: 4/12 Oblique: 2 With the rule: 2	Ipsilateral: 0/12
	Contralateral: 3/12 Oblique: 1 With the rule: 2	Contralateral: 1/12 Oblique: 0 With the rule: 1
Anisometropia of SE ≥ 1D	2/12	2/12 New onset: 1
Astigmatic anisometropia ≥ 1D	3/12	1/12
Subnormal vision	Ipsilateral: 0/12	Ipsilateral: 0/12
	Contralateral: 2/12	Contralateral: 4/12 New onset: 2
Symmetry (%)	84 ± SD 2 (range 80–88)	86 ± SD 3 (range 81–90)
Globe:orbit volume ratio (%)	Ipsilateral: 38 ± SD 5 (range 31–50)	Ipsilateral: 36 ± SD 5 (range 28–44)
	Contralateral: 39 ± SD 6 (range 30–50)	Contralateral: 35 ± SD 5 (range 28–43)

CT: computed tomography; D: diopter; n: number; SD: standard deviation; SE: spherical equivalent.

Ethics

The study was approved by the Ethical Review Board of Uppsala, Sweden (2017/452) and was performed in accordance with the Declaration of Helsinki.

Results

Twelve patients (8 female and 4 male) were included in the study. Nine patients had right-sided UCS and 3 left-sided UCS. The mean age at surgery was 12 ± SD 5 (range 9–26) months. At follow-up, 4 patients had new-onset strabismus on the ipsilateral side and 3 on the contralateral side. Thus, more than half of the patients developed strabismus during the postoperative phase. Ages, ophthalmological outcome, symmetry, and globe:orbit volume ratios are given in Table 1.

Nine patients improved in orbital symmetry (range 1–6%), 2 did not improve (0%), and 1 patient had decreased 1% in symmetry by follow-up (Table 2). The mean improvement in orbital symmetry was 2%. The globe:orbit volume ratio was smaller on the ipsilateral compared to the contralateral side in 6/12 children preoperatively and at follow-up in 8/12. On the ipsilateral side, the globe:orbit volume ratio had decreased in 9/12 children by follow-up, with a mean decrease of 2.2 (range -7.4 to +6.3) % (Table 2). On the contralateral side, the globe:orbit volume ratio had decreased in 9/12 children with a mean decrease of 3.3 (range -6.9 to +10.2) %. In 3 children with an increase in the globe:orbit volume ratio, 2 children had increase on both eyes, 1 only ipsilaterally, and 1 only on the contralateral side. Distance maps of orbits preoperatively and at follow-up for each patient are illustrated in Figure 3. PCA of each of the four groups resulted in shape variations illustrated in Figure 4.

Morphology, volume, and ophthalmological outcome

The relation between improvement in symmetry and new-onset strabismus is summarized in Table 2 and Figure 5A. Preoperative contralateral strabismus was associated with PC1- (large, diagonal shape) and lower globe:orbit volume ratio. Ipsilaterally at follow-up, no clear correlation was found between morphology, globe:orbit volume ratio, and strabismus. However, contralateral strabismus at follow-up was associated with PC1- (oval/vertically compressed shape) and a higher globe:orbit volume ratio.

Regarding hypermetropia, on the ipsilateral side both preoperatively and at follow-up, PC3- and PC3+ (both representing different variations of Harlequin deformity with a vertically elongated/horizontally compressed shape or a round and superiorly compressed shape) were associated with hypermetropia. On the contralateral side, no clear relation was identified preoperatively but at follow up, PC2- (diagonal shape) and PC2+ (round and small shape) were associated with hypermetropia. Regarding globe:orbit volume ratio, no clear correlation to hypermetropia was found in any group. No relations between symmetry or globe:orbit volume ratio and anisometropia of SE were identified.

Children who improved in orbital symmetry also tended to improve in astigmatic anisometropia (Figure 5B). Preoperatively, children with more asymmetric orbits also had more astigmatic anisometropia. Regarding astigmatism preoperatively, on the ipsilateral side, PC1 and PC2 (variations of Harlequin deformity with a vertically elongated/horizontally compressed shape) were associated with astigmatism. Ipsilateral PC1 preoperatively was associated with the axis of astigmatism, where PC1- (variations of Harlequin deformity with a vertically elongated/horizontally compressed shape) as well as a small globe:orbit volume ratio was related to astigmatism with the rule, and PC1+ (round, small shape) and a large globe:orbit volume ratio were associated with oblique astigmatism (Figure 5C). On the contralateral side preoperatively, PC1- (large, diagonal shape) and PC1+ (round, small shape) were associated with astigmatism. At follow-up, the one patient with significant astigmatism had it on the contralateral side and also had the largest globe:orbit volume ratio of the group.

Two children had subnormal vision preoperatively on the contralateral side, which remained at follow-up and was due to astigmatic anisometropia in combination with strabismus in one case

and due to strabismus in the other case. No association between morphology or volume and subnormal vision was found preoperatively. At follow-up, two new cases of subnormal vision were found, in one case due to new-onset strabismus and in another due to anisometropia of SE in combination with new-onset strabismus. At follow-up, contralateral PC1- (oval/vertically compressed shape) as well as a higher globe:orbit volume ratio was related to subnormal vision.

Discussion

In this study, ophthalmological manifestations were related to variation and improvement in orbital morphology and globe:orbit volume ratio after FOAR and subsequent orbital growth. Deformed orbital shapes and improvement in symmetry after FOAR were associated with ophthalmological manifestations. Different mechanisms seemed to cause strabismus pre- and postoperatively, and FOAR did not seem to sufficiently correct the orbit. These findings may have implications for tailored ophthalmological follow-up, and further development of surgical treatments aimed at improved bilateral correction of orbital morphology and volume relations.

Improvement in orbital symmetry at follow-up results from the surgical correction of FOAR and subsequent growth. In this study, improvement in symmetry was associated with new onset strabismus when investigating both the ipsilateral and contralateral sides. However, when examining individual cases, the association was not very strong. In a previous study, the authors hypothesized that patients with a more severe orbital deformity preoperatively, therefore in need of more correction at surgery, were at higher risk of developing strabismus [9]. The main reason for presumed induced iatrogenic strabismus is speculated to be the periorbital dissection and repositioning of the trochlea that FOAR entails [6, 9, 12]. Larger corrections lead to greater displacement of the trochlea, more significant changes in orbital anatomy, and an altered position of the extraocular muscles (EOM), as discussed by previous authors [24], which could explain a higher prevalence of strabismus. However, new-onset strabismus was associated with lack of improvement in symmetry in two patients. This could be due to the small sample size or perhaps implying that investigation of additional factors is necessary to fully understand strabismus after FOAR.

Preoperative contralateral strabismus was associated with a lower globe:orbit volume ratio and a large diagonal orbit. Possibly, the relatively smaller globe could lead to rotation of both the globe and the recti EOM, resulting in changes in the muscles course of action and subsequent strabismus. Conversely, at follow-up, strabismus on the contralateral side was associated with a higher globe:orbit volume ratio and oval/vertically compressed orbital shape, implying different mechanisms behind EOM imbalance pre- and postoperatively on the contralateral side. No contralateral orbits were distinctively oval preoperatively, but it is not known to which degree contralateral orbital morphology was influenced by the surgery. In summary, these findings implicate that strabismus is a bilateral issue in UCS and that there might be different mechanisms behind pre- and postoperative contralateral strabismus. Consequently, improved correction of the orbits bilaterally than what was achieved here with FOAR might be needed to avoid functional issues.

Vertically elongated orbital shape tended to associate with hypermetropia on the ipsilateral side preoperatively that persisted after surgery. On the contralateral side, no relations were found preoperatively, but at follow-up, children with a diagonal or round and small orbit were more hypermetropic. The hypermetropic eye has a shorter axial length; infants are therefore usually more hypermetropic initially, but the refractive error tends to decrease with growth following a process known as emmetropization [25]. We can hypothesize that changes in orbital morphology pre- and postoperatively could interfere with the ocular growth and thus the axial length, resulting in hypermetropia.

Based on this study, the typical ipsilateral deformity corresponding to the Harlequin deformity, irrespective of its severity, seems to result in ipsilateral astigmatism, adding to the argument that optimal morphological correction of the orbit is important to avoid functional issues. On the contralateral side, however, a rather ordinary shape

Table 2. New onset strabismus, asymmetry, and globe:orbit volume ratio per patient.

Patient ID	Symmetry (Dice in %)		Globe/(globe+orbit) volume (%)		New-onset strabismus postop		Strabismus preop and postop		No strabismus preop or postop	
	Preop	Postop	Preop	Postop	Ipsi	Contra	Ipsi	Contra	Ipsi	Contra
I	80	81	Ipsi: 37 Contra: 39	Ipsi: 43 Contra: 39	-	-	-	-	X	X
II	81	85	Ipsi: 50 Contra: 50	Ipsi: 44 Contra: 39	-	-	-	-	X	X
III	82	85	Ipsi: 38 Contra: 40	Ipsi: 36 Contra: 33	X	-	-	-	-	X
IV	84	85	Ipsi: 36 Contra: 31	Ipsi: 34 Contra: 33	-	-	-	X	X	-
V	84	89	Ipsi: 40 Contra: 43	Ipsi: 33 Contra: 32	-	-	-	-	X	X
VI	85	85	Ipsi: 35 Contra: 33	Ipsi: 28 Contra: 32	-	X	-	-	X	-
VII	84	84	Ipsi: 31 Contra: 36	Ipsi: 34 Contra: 35	X	X	-	-	-	-
VIII	86	90	Ipsi: 45 Contra: 44	Ipsi: 41 Contra: 41	-	-	-	X	X	-
IX	85	84	Ipsi: 40 Contra: 43	Ipsi: 39 Contra: 37	-	-	-	-	X	X
X	88	90	Ipsi: 36 Contra: 39	Ipsi: 38 Contra: 43	-	-	-	-	X	X
XI	82	88	Ipsi: 32 Contra: 30	Ipsi: 29 Contra: 28	X	X	-	-	-	-
XII	85	85	Ipsi: 38 Contra: 37	Ipsi: 33 Contra: 32	X	-	-	X	-	-

Dice: Dice similarity coefficient; Ipsi: ipsilateral; Contra: contralateral; preop: preoperative; postop: postoperative.

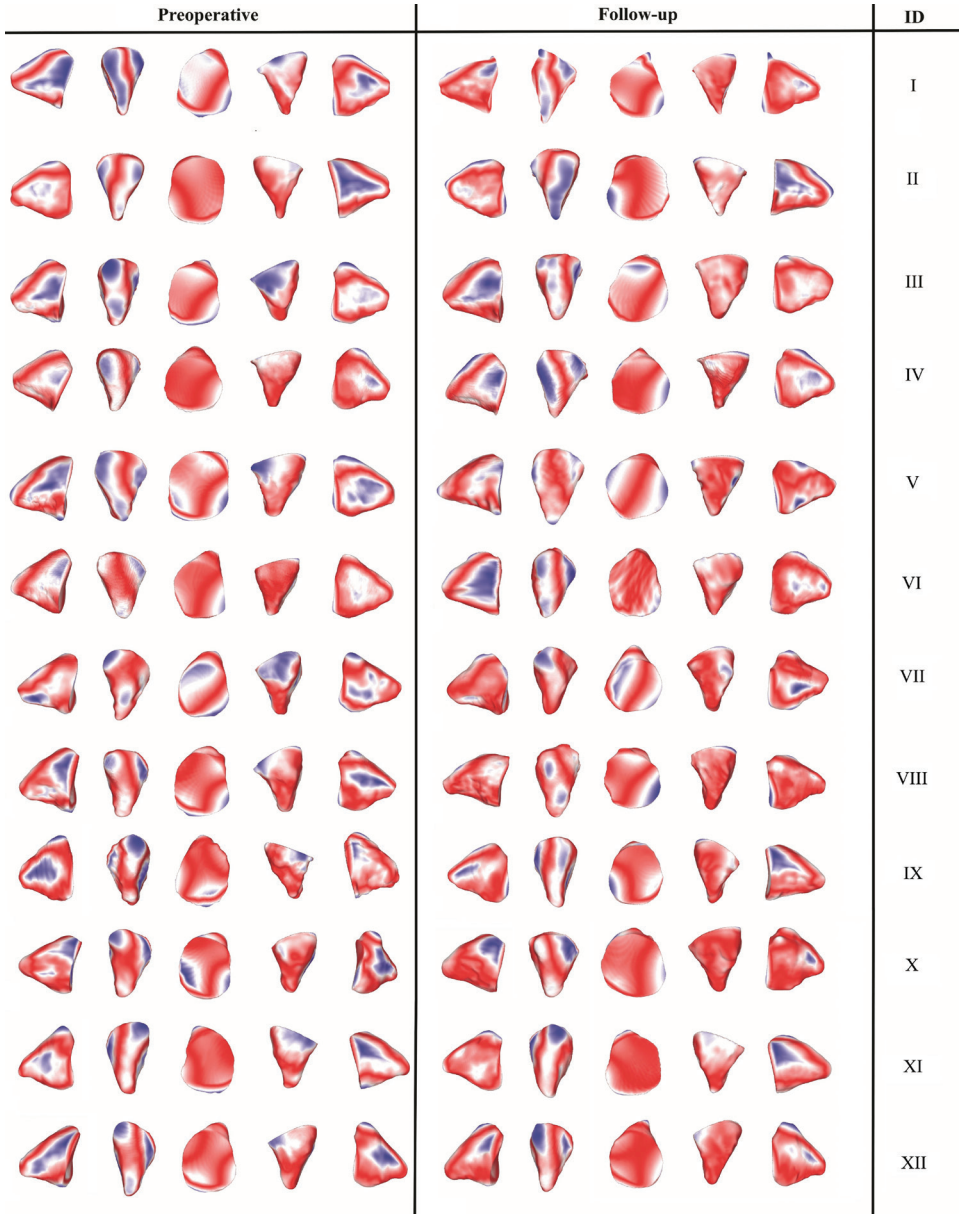

Figure 3. Distance maps comparing ipsilateral and contralateral orbits. Shapes of ipsilateral orbits are visualized. Blue indicates that the contralateral orbit is locally smaller, red indicates the opposite, and white indicates no local difference. Preoperative orbits to the left, orbits at follow-up to the right, and subject number to the very right.

was associated with astigmatism. Possibly, different mechanisms could cause ipsi- and contralateral astigmatism. Regarding the axis of astigmatism, explicit Harlequin deformity as characterized by elevation of the superolateral corner of the orbit leading to higher vertical axis could potentially influence the curvature of the eye, thereby inducing astigmatism with the rule. A small globe:orbit volume ratio was associated with astigmatism with the rule and the opposite with oblique astigmatism. Generally, both orbits are smaller in UCS compared to healthy controls [9, 13], which could potentially influence the globe and induce oblique astigmatism, as supported by the findings of this study. The way orbital shape affects corneal curvature is complex; future studies including analyses of the globe position in relation to the orbit could elucidate this further.

Astigmatic anisometropia in UCS has been well described in the literature [1, 4, 5, 8]. It is speculated to result from an abnormal and asymmetric orbital shape. Therefore, improvement in orbital symmetry after surgery could decrease the prevalence of astigmatism and anisometropia. The above is in accordance with this study. Children with more asymmetric orbits preoperatively tended to have more astigmatic anisometropia. Further, the children who improved most in orbital symmetry after surgery were those who also improved in anisometropia. On the contrary, they also had a higher prevalence of new-onset strabismus, adding to the complexity of optimal orbital reconstruction in UCS.

Anisometropia in refractive error as well as strabismus in the pediatric population predisposes subnormal vision and amblyopia. In the present study, no cases of subnormal vision were found on the ipsilateral side at any time point. Two cases were documented on the contralateral side preoperatively and four at follow-up, related to strabismus or strabismus in combination with anisometropia. An oval/vertical compressed orbital shape seemed to relate to subnormal vision. The same shape was also associated with strabismus. In addition, a larger globe:orbit volume ratio was associated with subnormal vision, especially in cases of new onset subnormal vision.

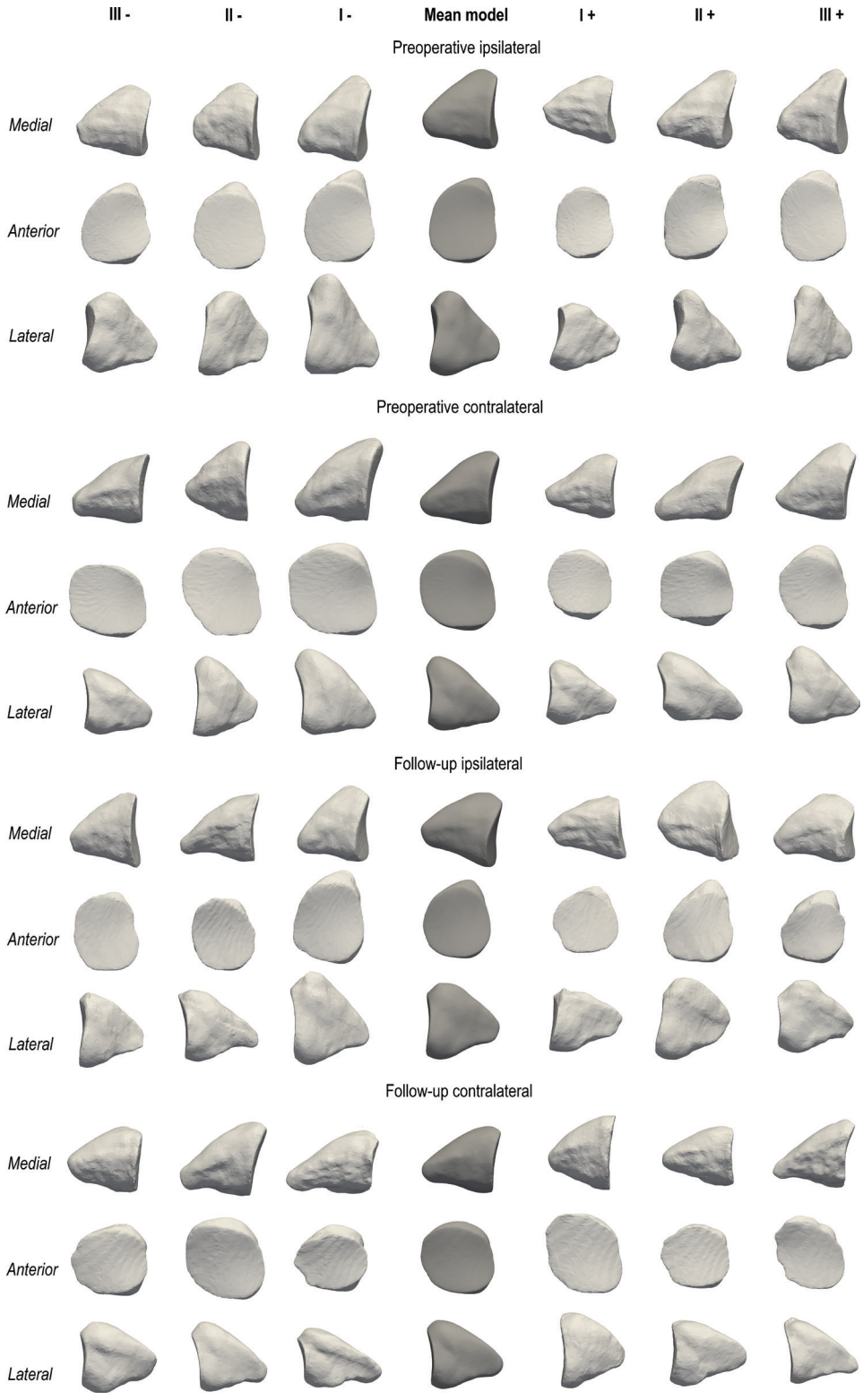

Figure 4. Principal component analysis. Four groups from above: preoperative ipsilateral, preoperative contralateral, follow-up ipsilateral, and follow-up contralateral. Mean model for each group in the middle (dark grey), negative modes to the left, positive modes to the right. Three projections of each mode from above: medial, anterior, lateral. I+: positive first principal mode; I-: negative first principal mode; II+: positive second principal mode; II-: negative second principal mode; III+: positive third principal mode; III-: negative third principal mode.

A larger ratio was also related to contralateral strabismus at follow-up in this study. This could indicate that certain orbital morphological variations and globe:orbit relations are predisposing ophthalmological symptoms, which could be of importance in predicting long-term ophthalmological outcomes and designing optimal surgical treatment protocols. It is important to identify children with subnormal vision to treat and prevent amblyopia; future studies predicting outcomes could lead to improved care for high-risk patients.

In this study, the prevalence of astigmatism, astigmatic anisometropia, and ipsilateral strabismus both pre- and postoperatively was lower

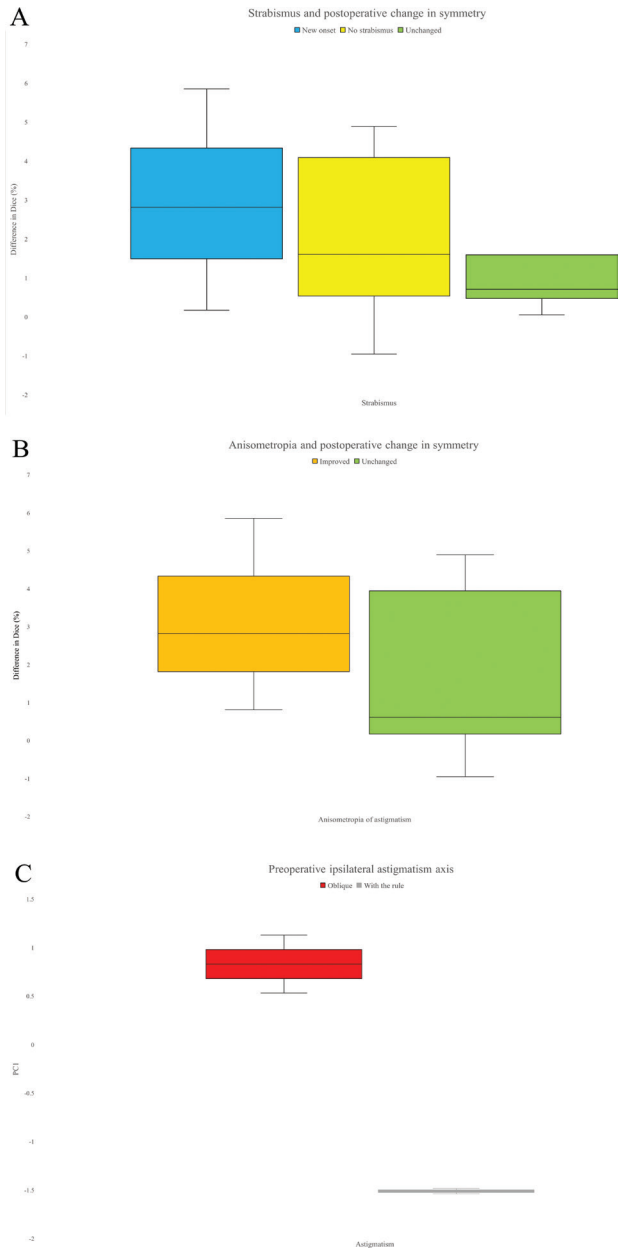

Figure 5. (A) Postoperative change in symmetry and strabismus comparing patients with new onset strabismus (blue), patients who never had strabismus at any time point (yellow), and patients who had strabismus both preoperatively and at follow-up (green). (B) Postoperative change in symmetry and anisometropia of astigmatism, comparing patients who improved in anisometropia (orange) to patients who had unchanged anisometropia (green). (C) Preoperative axis of astigmatism and variations in orbital shape preoperatively on the ipsilateral side. Oblique astigmatism (red) is associated with positive aspects of the first principal component, and astigmatism with the rule (gray) is associated with negative aspects of the first principal component. Dice: Dice similarity coefficient; PC1: first principal component.

compared to previous studies [1, 4, 5, 7, 12, 26–28]. This discrepancy might likely be explained by the small cohort size. The greatest limitation of the study was the small cohort size, which was partly due to that only patients with complete qualitative examinations were included to minor the bias to the largest extent possible. The purely qualitative design was also due to the limited sample. Other limitations included lack of imaging at age 5, which was avoided for ethical reasons related to radiation exposure, as well as manual placement of landmark to define the anterior limitation of the orbit. Additionally, not all principal components explaining the variance were included; however, that was not feasible for reasons outlined in the methods section. On the other hand, standardized ophthalmological examinations were comprehensive and performed at set time points with only small variations in age. No controls were included; however, only validated measures were used. Larger studies including objective 3D morphological analyses and qualitative standardized ophthalmological examinations are needed to better understand the complex relation between orbital morphology and functional problems in UCS.

Acknowledgements

The authors would like to thank the research group member Johan Nysjö PhD for laying foundations to develop software, workflows, and open source code enabling this study and orthoptists Jenny Bjuhr, Sofia Ferngren, and Jonina Hreinsdottir for their help with orthoptic examinations.

Contributors

All authors meet the authorship criteria. No others meeting the criteria were omitted. All authors contributed to the study conception and design, interpretation of analyses, revising, and final approval of the article. HL contributed to data acquisition, analyses, drafting the article, and development of the workflow for image analysis based on previous work from Johan Nysjö PhD. EN contributed to extensive data acquisition and drafting the article. HL and EN contributed equally to the study, thereby motivating shared first authorship. EL and DN contributed equally and took shared senior responsibility of the study, thereby motivating shared last authorship.

Funding

This study was funded by Ögonfonden, Stiftelsen Kronprinsessan Margaretas Arbetsnämnd för Synskadade, Synskadades vänner in Uppsala County, ALF grants Region Uppsala. No funders were involved in the study design, data collection, analyses, interpretation of data, writing the manuscript, or in the decision to submit this paper.

Competing interests

Nothing to declare.

ORCID

Hanna Lif https://orcid.org/0009-0000-5562-0942
Evangelia Ntoula https://orcid.org/0009-0007-6444-2034
Eva Larsson https://orcid.org/0000-0001-9674-0094
Daniel Nowinski https://orcid.org/0000-0002-8371-9314

References

[1] Touzé R, Paternoster G, Arnaud E, et al. Ophthalmological findings in children with unicoronal craniosynostosis. Eur J Ophthalmol. 2022;32(6):3274–3280. https://doi.org/10.1177/11206721221077548
[2] Ntoula E, Nowinski D, Holmstrom G, et al. Ophthalmological findings in children with non-syndromic craniosynostosis: preoperatively and postoperatively up to 12 months after

surgery. BMJ Open Ophthalmol. 2021;6(1):e000677. https://doi.org/10.1136/bmjophth-2020-000677

[3] Di Rocco C, Paternoster G, Caldarelli M, et al. Anterior plagiocephaly: epidemiology, clinical findings, diagnosis, and classification: a review. Childs Nerv Syst. 2012;28(9):1413–1422. https://doi.org/10.1007/s00381-012-1845-2

[4] Luo W-T, Chen X, Zhang Y-D, et al. Ophthalmological outcomes of unilateral coronal synostosis in young children. BMC Ophthalmol. 2020;20(1):318. https://doi.org/10.1186/s12886-020-01547-1

[5] Levy RL, Rogers GF, Mulliken JB, et al. Astigmatism in unilateral coronal synostosis: incidence and laterality. J AAPOS. 2007;11(4):367–372. https://doi.org/10.1016/j.jaapos.2007.02.017

[6] Samra F, Paliga JT, Tahiri Y, et al. The prevalence of strabismus in unilateral coronal synostosis. Childs Nerv Syst. 2015;31(4):589–596. https://doi.org/10.1007/s00381-014-2580-7

[7] Gencarelli JR, Murphy A, Samargandi OA, et al. Ophthalmologic outcomes following fronto-orbital advancement for unicoronal craniosynostosis. J Craniofac Surg. 2016;27(7):1629–1635. https://doi.org/10.1097/SCS.0000000000003085

[8] Ntoula E, Nowinski D, Holmström G, et al. Strabismus and refraction in non-syndromic craniosynostosis – a longitudinal study up to 5 years of age. Acta Ophthalmol. 2024;102(5):564–572. https://doi.org/10.1111/aos.16605

[9] Yu JW, Xu W, Wink JD, et al. Strabismus in unicoronal craniosynostosis: effect of orbital dysmorphology and fronto-orbital advancement and remodeling. Plast Reconstr Surg.2020;145(2):382e–390e.https://doi.org/10.1097/PRS.0000000000006479

[10] Villavisanis DF, Blum JD, Cho DY, et al. Long-term aesthetic and photogrammetric outcomes in non-syndromic unicoronal synostosis: comparison of fronto-orbital distraction osteogenesis and fronto-orbital advancement and remodeling. Childs Nerv Syst. 2023;39(5):1283–1296. https://doi.org/10.1007/s00381-023-05857-9

[11] Alford J, Derderian CA, Smartt JM, Jr. Surgical treatment of nonsyndromic unicoronal craniosynostosis. J Craniofac Surg. 2018;29(5):1199–1207. https://doi.org/10.1097/SCS.0000000000004509

[12] Elhusseiny AM, MacKinnon S, Zurakowski D, et al. Long-term ophthalmic outcomes in 120 children with unilateral coronal synostosis: a 20-year retrospective analysis. J AAPOS. 2021;25(2):76.e1–76.e5. https://doi.org/10.1016/j.jaapos.2020.10.013

[13] Lif, H. M., Nysjö, J. E., Vegelius, J. R., Unander-Scharin, J., Enblad, P., & Nowinski, D. J. (2023). Persistent discrepancies in orbital morphology after surgical treatment of unicoronal craniosynostosis: a critical image-based analysis. Journal of neurosurgery. Pediatrics, 1–10. Advance online publication. https://doi.org/10.3171/2023.1.PEDS22349

[14] Levasseur J, Nysjö J, Sandy R, et al. Orbital volume and shape in Treacher Collins syndrome. J Craniomaxillofac Surg. 2018;46(2):305–311. https://doi.org/10.1016/j.jcms.2017.11.028

[15] Khonsari RH, Hennocq Q, Nysjö J, et al. Defining critical ages for orbital shape changes after frontofacial advancement in crouzon syndrome. Plast Reconstr Surg. 2019;144(5):841e–852e. https://doi.org/10.1097/PRS.0000000000006162

[16] Bellaire CP, Devarajan A, Napoli JG, et al. Craniofacial dysmorphology in infants with non-syndromic unilateral coronal craniosynostosis. J Craniofac Surg. 2022;33(6):1903–1908. https://doi.org/10.1097/SCS.0000000000008464

[17] Ramdat Misier KRR, Breakey RWF, van de Lande LS, et al. Correlation between head shape and volumetric changes following spring-assisted posterior vault expansion. J Craniomaxillofac Surg. 2022;50(4):343–352. https://doi.org/10.1016/j.jcms.2021.05.004

[18] Pluijmers BI, Ponniah AJ, Ruff C, et al. Using principal component analysis to describe the Apert skull deformity and simulate its correction. J Plast Reconstr Aesthet Surg. 2012;65(12):1750–1752. https://doi.org/10.1016/j.bjps.2012.07.007

[19] Srivilasa C, Zhao L, Patel PK, et al. Statistical shape analysis of metopic craniosynostosis: a preliminary study. Conf Proc IEEE Eng Med Biol Soc. 2006;2006:4066–4069. https://doi.org/10.1109/IEMBS.2006.260032

[20] Staal FC, Ponniah AJ, Angullia F, et al. Describing Crouzon and Pfeiffer syndrome based on principal component analysis. J Craniomaxillofac Surg. 2015;43(4):528–536. https://doi.org/10.1016/j.jcms.2015.02.005

[21] Way BLM, Khonsari RH, Karunakaran T, et al. Correcting exorbitism by monobloc frontofacial advancement in Crouzon-Pfeiffer syndrome: an age-specific, time-related, controlled study. Plast Reconstr Surg. 2019;143(1):121e–132e. https://doi.org/10.1097/PRS.0000000000005105

[22] Nysjö J. Interactive 3D image analysis for cranio-maxillofacial surgery planning and orthopedic applications. Acta Universitatis Upsaliensis; 2016.

[23] Yushkevich PA, Piven J, Hazlett HC, et al. User-guided 3D active contour segmentation of anatomical structures: significantly improved efficiency and reliability. Neuroimage. 2006;31(3):1116–1128.https://doi.org/10.1016/j.neuroimage.2006.01.015

[24] Hoppe IC, Taylor JA. A cohort study of strabismus rates following correction of the unicoronal craniosynostosis deformity: conventional bilateral fronto-orbital advancement versus fronto-orbital distraction osteogenesis. J Craniofac Surg. 2021;32(7):2362–2365. https://doi.org/10.1097/SCS.0000000000007773

[25] Mayer DL, Hansen RM, Moore BD, et al. Cycloplegic refractions in healthy children aged 1 through 48 months. Arch Ophthalmol. Uppsala. 2001;119(11):1625–1628. https://doi.org/10.1001/archopht.119.11.1625

[26] Macintosh C, Wall S, Leach C. Strabismus in unicoronal synostosis: ipsilateral or contralateral? J Craniofac Surg. 2007;18(3):465–469. https://doi.org/10.1097/scs.0b01e3180515d94

[27] Song HB, Yang HK, Baek RM, et al. Effect of fronto-orbital advancement on astigmatism in patients with anterior plagiocephaly. J Craniomaxillofac Surg. 2016;44(10):1504–1507. https://doi.org/10.1016/j.jcms.2016.04.028

[28] Tarczy-Hornoch K, Smith B, Urata M. Amblyogenic anisometropia in the contralateral eye in unicoronal craniosynostosis. J AAPOS. 2008;12(5):471–476. https://doi.org/10.1016/j.jaapos.2008.03.008